NEW DIFFRACTION DATA

Crystal structure of deracoxib, $C_{17}H_{14}F_3N_3O_3S$

James A. Kaduk [ORCID],[1,2,a)] Amy M. Gindhart [ORCID],[3] Stacy Gates-Rector [ORCID],[3] and Thomas N. Blanton [ORCID][3]

[1]Illinois Institute of Technology, 3101 S. Dearborn St., Chicago, IL 60616, USA
[2]North Central College, 131 S. Loomis St., Naperville, IL 60540, USA
[3]ICDD, 12 Campus Blvd., Newtown Square, PA 19073-3273, USA

The crystal structure of deracoxib has been solved and refined using synchrotron X-ray powder diffraction data, and optimized using density functional theory techniques. Deracoxib crystallizes in space group *Pbca* (#61) with $a = 9.68338(11)$, $b = 9.50690(5)$, $c = 38.2934(4)$ Å, $V = 3525.25(3)$ Å^3, and $Z = 8$. The molecules stack in layers parallel to the *ab*-plane. N–H⋯O hydrogen bonds link the molecules along the *b*-axis, in chains with the graph set *C1,1(4)*, as well as more-complex patterns. N–H⋯N hydrogen bonds link the layers. The powder pattern has been submitted to ICDD for inclusion in the Powder Diffraction File™ (PDF®).
© The Author(s), 2023. Published by Cambridge University Press on behalf of International Centre for Diffraction Data. This is an Open Access article, distributed under the terms of the Creative Commons Attribution licence (http://creativecommons.org/licenses/by/4.0/), which permits unrestricted re-use, distribution and reproduction, provided the original article is properly cited.
[doi:10.1017/S0885715622000525]

I. INTRODUCTION

Deracoxib (sold under the brand name Deramaxx) is a selective cyclooxygenase 2 inhibitor, used in veterinary medicine for the control of pain and inflammation associated with osteoarthritis in dogs. Deracoxib is also used after canine dental procedures and is not recommended for use in cats. The systematic name (CAS Registry Number 169590-41-4) is 4-[3-(difluoromethyl)-5-(3-fluoro-4-methoxyphenyl)pyrazol-1-yl]benzenesulfonamide. A two-dimensional molecular diagram is shown in Figure 1.

We are unaware of any published powder diffraction data on deracoxib. This work was carried out as part of a project (Kaduk et al., 2014) to determine the crystal structures of large-volume commercial pharmaceuticals, and include high-quality powder diffraction data for them in the Powder Diffraction File (Gates-Rector and Blanton, 2019).

II. EXPERIMENTAL AND REFINEMENTS

Deracoxib was a commercial reagent, purchased from TargetMol (Batch #113281), and was used as-received. The white powder was packed into a 1.5 mm diameter Kapton capillary and rotated during the measurement at ~50 Hz. The powder pattern was measured at 295 K at beamline 11-BM (Antao et al., 2008; Lee et al., 2008; Wang et al., 2008) of the Advanced Photon Source at Argonne National Laboratory using a wavelength of 0.458208(2) Å from 0.5 to 50° 2θ with a step size of 0.001° and a counting time of 0.1 s step^{-1}. The high-resolution powder diffraction data were collected using twelve silicon crystal analyzers

that allow for high angular resolution, high precision, and accurate peak positions. A mixture of silicon (NIST SRM 640c) and alumina (NIST SRM 676a) standards (ratio Al_2O_3:Si = 2:1 by weight) was used to calibrate the instrument and refine the monochromatic wavelength used in the experiment.

The pattern was indexed using JADE Pro 8.1 (MDI, 2021) on a high-quality primitive orthorhombic unit cell with $a = 9.71606$, $b = 9.54339$, $c = 38.43565$ Å, $V = 3563.91$ Å^3, and $Z = 8$. The suggested space group was *Pbca*, which was confirmed by successful solution and refinement of the structure. A reduced cell search in the Cambridge Structural Database (Groom et al., 2016) combined with only C, H, F, N, O, and S elements, yielded no hits.

A deracoxib molecule was downloaded from PubChem (Kim et al., 2019) as Conformer3D_CID_3058754.sdf. It was converted to a *.mol2 file using Mercury (Macrae et al., 2020) and to a Fenske-Hall Z-matrix using Open Babel (O'Boyle et al., 2011). The structure was solved using FOX (Favre-Nicolin and Černý, 2002) using $\sin\theta/\lambda_{max} = 0.32$ Å^{-1} ($2\theta_{max} = 16.9°$).

Rietveld refinement was carried out using GSAS-II (Toby and Von Dreele, 2013). Only the 1.0–25.0° portion of the pattern was included in the refinement ($d_{min} = 1.058$ Å). The region 1.50–2.12°, which contained a peak from the Kapton capillary, was excluded from the refinement. All non-H bond distances and angles were subjected to restraints, based on a Mercury/Mogul Geometry Check (Bruno et al., 2004; Sykes et al., 2011). The Mogul average and standard deviation for each quantity were used as the restraint parameters. The restraints contributed 4.2% to the final χ^2. The hydrogen atoms were included in calculated positions, which were recalculated during the refinement using Materials Studio (Dassault, 2021).

a)Author to whom correspondence should be addressed. Electronic mail: kaduk@polycrystallography.com

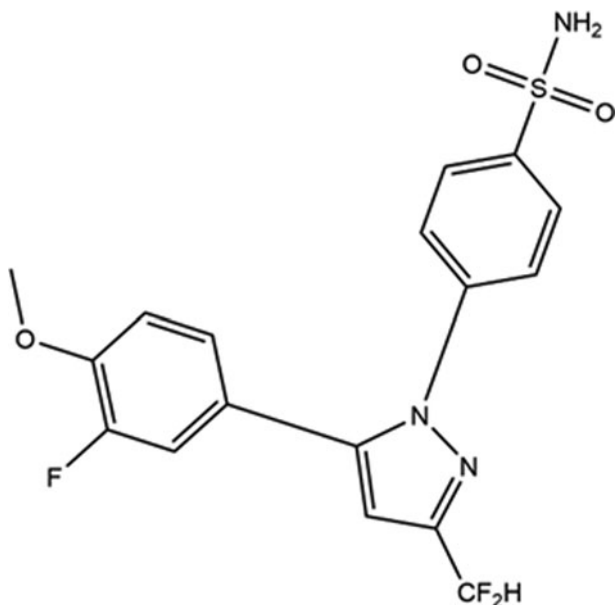Figure 1.   The 2D molecular structure of deracoxib.

in the difference plot (Figure 2) are in the shapes of some of the strong low-angle peaks.

The structure of deracoxib was optimized using VASP (Kresse and Furthmüller, 1996) (fixed experimental unit cell) through the MedeA graphical interface (Materials Design, 2016). The calculation was carried out on 16 2.4 GHz processors (each with 4 GB RAM) of a 64-processor HP Proliant DL580 Generation 7 Linux cluster at North Central College. The calculation used the GGA-PBE functional, a plane wave cutoff energy of 400.0 eV, and a k-point spacing of 0.5 Å^{-1} leading to a $2 \times 2 \times 1$ mesh, and took ~17 h. A single-point density functional theory calculation (fixed experimental cell) and population analysis were carried out using CRYSTAL17 (Dovesi *et al.*, 2018). The basis sets for the H, C, N, and O atoms in the calculation were those of Gatti *et al.* (1994), and those for F and S were those of Peintinger *et al.* (2013). The calculations were run on a 3.5 GHz PC using 8 k-points and the B3LYP functional, and took ~3.1 h.

The U_{iso} were grouped by chemical similarity. The U_{iso} for the H atoms were fixed at 1.3× the U_{iso} of the heavy atoms to which they are attached. A second-order spherical harmonic model was included in the refinement. The texture index was 1.032(0). The peak profiles were described using the generalized microstrain model. The background was modeled using a 6-term shifted Chebyshev polynomial, plus a peak at 5.81° 2θ to model the scattering from the Kapton capillary and any amorphous component.

The final refinement of 106 variables using 23 413 observations and 72 restraints yielded the residuals $R_{wp} = 0.0589$ and GOF = 1.26. The largest peak (1.09 Å from C19) and hole (1.01 Å from C17) in the difference Fourier map were 0.19(5) and −0.23(5) eÅ^{-3}, respectively. The largest errors

III. RESULTS AND DISCUSSION

The root-mean-square (rms) Cartesian displacement between the Rietveld-refined and DFT-optimized structures of deracoxib is 0.070 Å (Figure 3). The excellent agreement provides strong evidence that the structure is correct (van de Streek and Neumann, 2014). This discussion concentrates on the DFT-optimized structure. The asymmetric unit (with atom numbering) is illustrated in Figure 4. The best view of the crystal structure is down the *a*-axis (Figure 5). The molecules stack in layers parallel to the *ab*-plane.

All of the bond distances and angles fall within the normal ranges indicated by a Mercury/Mogul Geometry Check (Macrae *et al.*, 2020). The quantum chemical geometry optimization of the deracoxib molecule (DFT/B3LYP/6-31G*/water) using Spartan '18 (Wavefunction, 2020) indicated that the observed conformation is very close to a local minimum in energy. A conformational analysis (MMFF
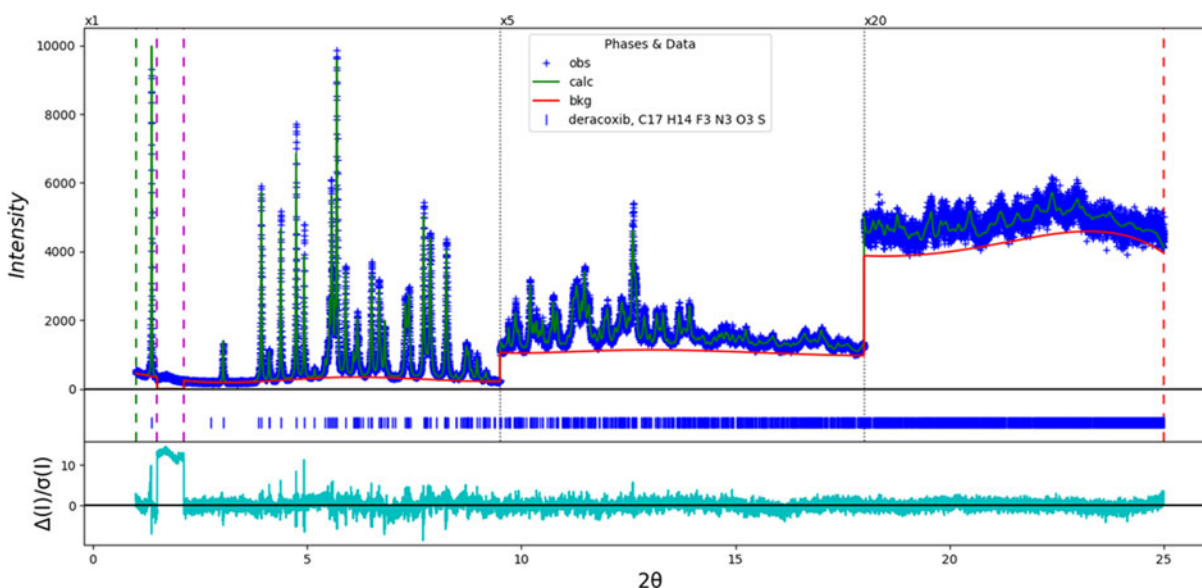

Figure 2.   The Rietveld plot for the refinement of deracoxib. The blue crosses represent the observed data points, and the green line is the calculated pattern. The cyan curve is the normalized error plot, and the red line is the background curve. The vertical scale has been multiplied by a factor of 5× for $2\theta > 9.5°$ and by 20× for $2\theta > 18.0°$. The two vertical magenta dashed lines indicate the excluded region 1.50–2.12° 2θ, which contains a peak from the Kapton capillary.
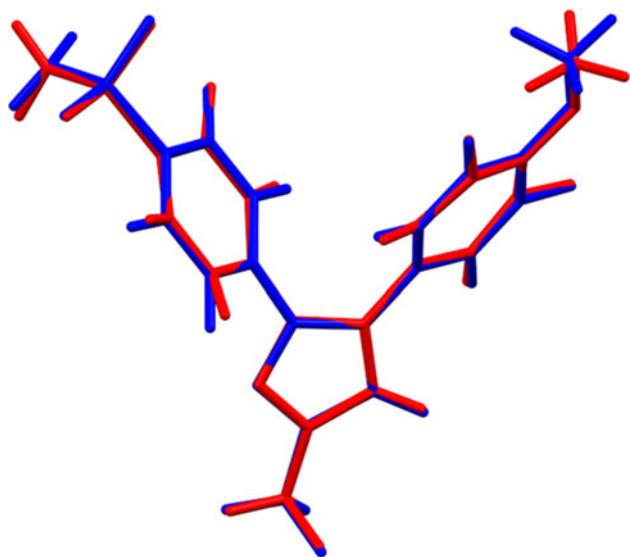
Figure 3. Comparison of the Rietveld-refined (red) and VASP-optimized (blue) structures of deracoxib. The rms Cartesian displacement is 0.070 Å. Image generated using Mercury (Macrae *et al.*, 2020).

force field) indicates that the minimum-energy conformation is 5.9 kcal mol^{-1} lower in energy, and has a different orientation of the phenyl ring containing the sulfonamide group (~180° rotation). Intermolecular interactions, thus, affect the solid-state conformation.

Analysis of the contributions to the total crystal energy of the structure using the Forcite module of Materials Studio (Dassault, 2021) suggests that the intramolecular deformation energy is dominated by angle deformation terms. The intermolecular energy is dominated by van der Waals and electrostatic attractions, which in this force field analysis also include hydrogen bonds. The hydrogen bonds are better analyzed using the results of the DFT calculation.

There are three traditional hydrogen bonds in the structure (Table I), between the amino group H37–N10–H38 and the sulfonyl group O6–S1–O7, as well as the ring nitrogen atom N9. The energies of the N–H⋯O hydrogen bonds were calculated using the correlation of Wheatley and Kaduk (2019). The N–H⋯O hydrogen bonds link the molecules along the *b*-axis, in chains with the graph set (Etter, 1990; Bernstein *et al.*, 1995; Shields *et al.*, 2000) *C1,1(4)*, as well as more-complex patterns. The N–H⋯N hydrogen bonds link the layers. Several intramolecular and intermolecular C–H⋯O and C–H⋯N hydrogen bonds contribute to the crystal energy.

The volume enclosed by the Hirshfeld surface of the deracoxib molecule (Figure 6; Hirshfeld, 1977; Turner *et al.*, 2017) is 433.26 Å^3, 98.32% of 1/8 the unit cell volume. The packing density is thus fairly typical. The only significant close contacts (red in Figure 6) involve the hydrogen bonds. The volume/non-hydrogen atom is 16.3 Å^3.

The Bravais–Friedel–Donnay–Harker (Bravais, 1866; Friedel, 1907; Donnay and Harker, 1937) morphology suggests that we might expect platy morphology for deracoxib, with {001} as the major faces. A second-order spherical harmonic model was included in the refinement. The texture index was 1.032(0), indicating that preferred orientation was small in this rotated capillary specimen.
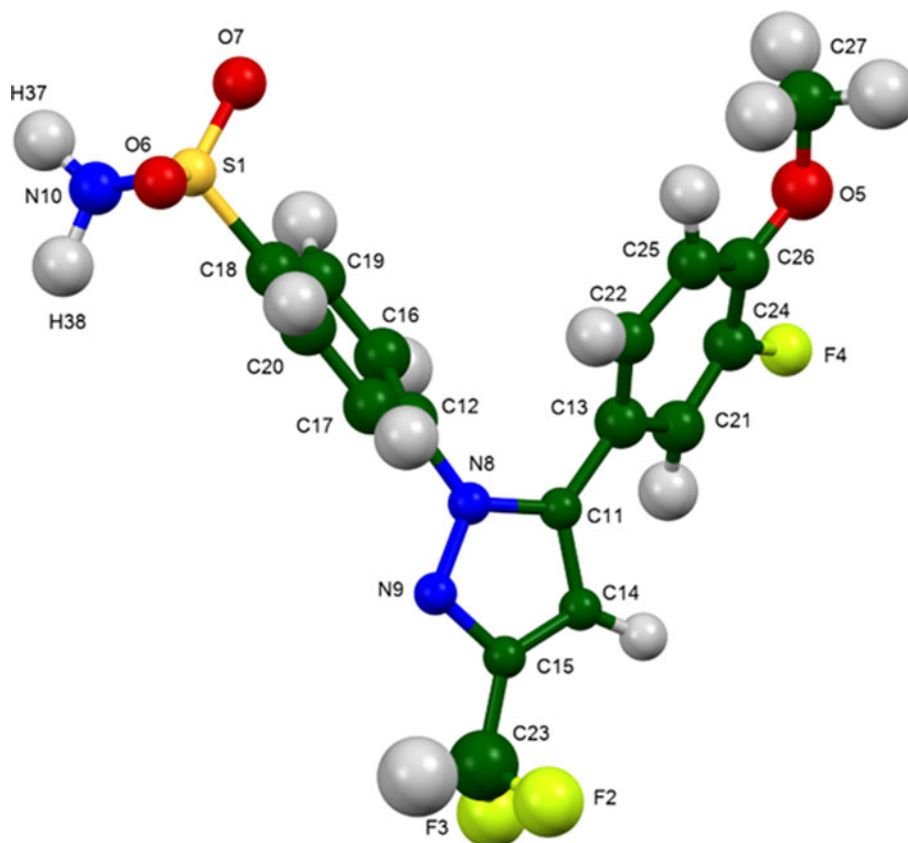

Figure 4. The asymmetric unit of deracoxib, with the atom numbering. The atoms are represented by 50% probability spheroids/ellipsoids. Image generated using Mercury (Macrae *et al.*, 2020).
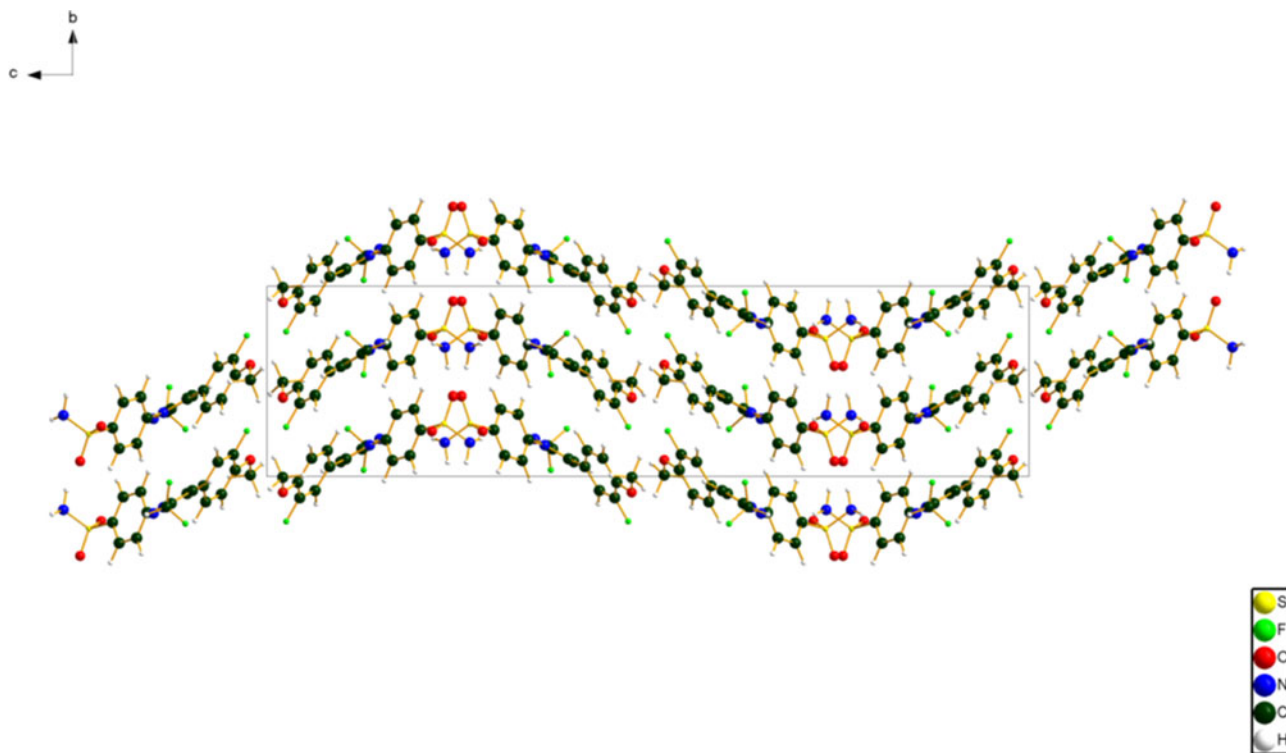
Figure 5. The crystal structure of deracoxib, viewed down the *a*-axis. Image generated using Diamond (Crystal Impact, 2022).

TABLE I. Hydrogen bonds (CRYSTAL17) in deracoxib.

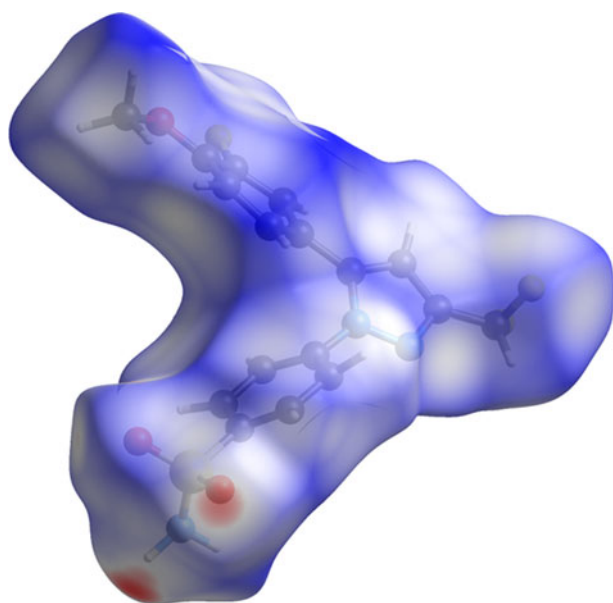| H-Bond	D-H (Å)	H···A (Å)	D···A (Å)	D-H···A (°)	Overlap (e)	E (kcal mol^{-1})
N10–H37···O6	1.032	1.811	2.797	158.7	0.054	5.4
N10–H38···O7	1.024	2.556	3.470	148.4	0.013	2.6
N10–H38···N9	1.024	2.715	3.347	120.0	0.012	
C23–H35···O7	1.099	2.302	3.370	163.3	0.023	
C16–H29···N9	1.091	2.747	3.805	163.1	0.016	
C20–H32···O6	1.089	2.410[a]	2.860	103.1	0.011	
C19–H31···O6	1.090	2.676	3.634	146.3	0.010	

[a]Intramolecular.

Figure 6. The Hirshfeld surface of deracoxib. Intermolecular contacts longer than the sums of the van der Waals radii are colored blue, and contacts shorter than the sums of the radii are colored red. Contacts equal to the sums of radii are white.

IV. DEPOSITED DATA

The powder pattern of deracoxib from this synchrotron data set has been submitted to ICDD for inclusion in the Powder Diffraction File. The Crystallographic Information Framework (CIF) files containing the results of the Rietveld refinement (including the raw data) and the DFT geometry optimization were deposited with the ICDD. The data can be requested at pdj@icdd.com.

CONFLICT OF INTEREST

The authors have no conflict of interest to declare.

REFERENCES

Antao, Sytle M., Ishmael Hassan, Jun Wang, Peter L. Lee, and Brian H. Toby. 2008. "State-of-the-Art High-Resolution Powder X-Ray Diffraction (HRPXRD) Illustrated with Rietveld Structure Refinement of Quartz, Sodalite, Tremolite, and Meionite." *The Canadian Mineralogist* 46 (6): 1501–9.

Bernstein, Joel, Raymond E. Davis, Liat Shimoni, and Ning-Leh Chang. 1995. "Patterns in Hydrogen Bonding: Functionality and Graph Set Analysis in Crystals." *Angewandte Chemie International Edition in English* 34 (15): 1555–73.

Bravais, Auguste. 1866. *Etudes Cristallographiques*. Paris, Gauthier-Villars.

Bruno, Ian J., Jason C. Cole, Magnus Kessler, Jie Luo, WD Sam Motherwell, Lucy H. Purkis, Barry R. Smith, Robin Taylor, Richard I. Cooper, Stephanie E. Harris, and A. Guy Orpen. 2004. "Retrieval of Crystallographically-Derived Molecular Geometry Information." *Journal of Chemical Information and Computer Sciences* 44 (6): 2133–44.

Crystal Impact. 2022. Diamond. V. 4.6.8. Crystal Impact - Dr. H. Putz & Dr. K. Brandenburg. Windows.

Dassault Systèmes. 2021. *Materials Studio 2021*. San Diego, CA, BIOVIA.

Donnay, J. D H., and David Harker. 1937. "A New Law of Crystal Morphology Extending the Law of Bravais." *American Mineralogist: Journal of Earth and Planetary Materials* 22 (5): 446–67.

Dovesi, Roberto, Alessandro Erba, Roberto Orlando, Claudio M. Zicovich-Wilson, Bartolomeo Civalleri, Lorenzo Maschio, Michel Rérat, Silvia Casassa, Jacopo Baima, Simone Salustro, and Bernard Kirtman. 2018. "Quantum-Mechanical Condensed Matter Simulations with CRYSTAL." *Wiley Interdisciplinary Reviews: Computational Molecular Science* 8 (4): e1360.

Etter, Margaret C. 1990. "Encoding and Decoding Hydrogen-Bond Patterns of Organic Compounds." *Accounts of Chemical Research* 23 (4): 120–6.

Favre-Nicolin, Vincent, and Radovan Černý. "FOX, 'Free Objects for Crystallography': A Modular Approach to ab initio Structure Determination from Powder Diffraction." *Journal of Applied Crystallography* 35 (6): 734–43.

Friedel, Georges. 1907. "Etudes sur la loi de Bravais." *Bulletin de Minéralogie* 30 (9): 326–455.

Gates-Rector, Stacy, and Thomas Blanton. 2019. "The Powder Diffraction File: A Quality Materials Characterization Database." *Powder Diffraction* 34 (4): 352–60.

Gatti, C., V. R. Saunders, and C. Roetti. 1994. "Crystal Field Effects on the Topological Properties of the Electron Density in Molecular Crystals: The Case of Urea." *The Journal of Chemical Physics* 101 (12): 10686–96.

Groom, C. R., Bruno, I. J., Lightfoot, M. P., and Ward, S. C. 2016. "The Cambridge Structural Database." *Acta Crystallographica Section B. Structural Science, Crystal Engineering and Materials* 72, 171–9.

Hirshfeld, Fred L. 1977. "Bonded-Atom Fragments for Describing Molecular Charge Densities." *Theoretica Chimica Acta* 44 (2): 129–38.

Kaduk, James A., Cyrus E. Crowder, Kai Zhong, Timothy G. Fawcett, and Matthew R. Suchomel. 2014. "Crystal Structure of Atomoxetine Hydrochloride (Strattera), C17H22NOCl." *Powder Diffraction* 29 (3): 269–73.

Kim, Sunghwan, Jie Chen, Tiejun Cheng, Asta Gindulyte, Jia He, Siqian He, Qingliang Li, Benjamin A. Shoemaker, Paul A. Thiessen, Bo Yu, Leonid Zaslavsky, Jian Zhang, and Evan E. Bolton. 2019. "PubChem 2019 Update: Improved Access to Chemical Data." *Nucleic Acids Research* 47 (D1): D1102–9. doi:10.1093/nar/gky1033.

Kresse, Georg, and Jürgen Furthmüller. 1996. "Efficiency of ab-initio Total Energy Calculations for Metals and Semiconductors Using a Plane-Wave Basis Set." *Computational Materials Science* 6 (1): 15–50.

Lee, Peter L., Deming Shu, Mohan Ramanathan, Curt Preissner, Jun Wang, Mark A. Beno, Robert B. Von Dreele, Lynn Ribaud, Charles Kurtz, Sytle M. Antao, Xuesong Jiao, and Brian H. Toby. 2008. "A Twelve-Analyzer Detector System for High-Resolution Powder Diffraction." *Journal of Synchrotron Radiation* 15 (5): 427–32.

Macrae, Clare F., Ioana Sovago, Simon J. Cottrell, Peter TA Galek, Patrick McCabe, Elna Pidcock, Michael Platings, Greg P. Shields, Joanna S. Stevens, Matthew Towler, and Peter A. Wood. 2020. "Mercury 4.0: From Visualization to Analysis, Design and Prediction." *Journal of Applied Crystallography* 53 (1): 226–35.

Materials Design Inc. 2016. *MedeA 2.20.4*. Angel Fire, NM, Materials Design Inc.

MDI Materials Data. 2022. JADE Pro Version 8.2. MDI Materials Data, Livermore, CA, USA.

O'Boyle, Noel M., Michael Banck, Craig A. James, Chris Morley, Tim Vandermeersch, and Geoffrey R. Hutchison. "Open Babel: An open chemical toolbox." *Journal of cheminformatics* 3, no. 1 (2011): 1–14.

Peintinger, Michael F., Daniel Vilela Oliveira, and Thomas Bredow. 2013. "Consistent Gaussian Basis Sets of Triple-Zeta Valence with Polarization Quality for Solid-State Calculations." *Journal of Computational Chemistry* 34 (6): 451–9.

Shields, Gregory P., Paul R. Raithby, Frank H. Allen, and WD Samuel Motherwell. 2000 "The Assignment and Validation of Metal Oxidation States in the Cambridge Structural Database." *Acta Crystallographica Section B: Structural Science* 56 (3): 455–65.

Sykes, Richard A., Patrick McCabe, Frank H. Allen, Gary M. Battle, Ian J. Bruno, and Peter A. Wood. 2011. "New Software for Statistical Analysis of Cambridge Structural Database Data." *Journal of Applied Crystallography* 44 (4): 882–6.

Toby, Brian H., and Robert B. Von Dreele. 2013. "GSAS-II: The Genesis of a Modern Open-Source all Purpose Crystallography Software Package." *Journal of Applied Crystallography* 46 (2): 544–9.

Turner, M. J., J. J. McKinnon, S. K. Wolff, D. J. Grimwood, P. R. Spackman, D. Jayatilaka, and M. A. Spackman. "CrystalExplorer17." (2017): 76730. http://hirshfeldsurface.net.

van de Streek, Jacco van de, and Marcus A. Neumann. 2014. "Validation of Molecular Crystal Structures from Powder Diffraction Data with Dispersion-Corrected Density Functional Theory (DFT-D)." *Acta Crystallographica. Section B, Structural Science, Crystal Engineering and Materials* 70 (Pt 6): 1020–32.

Wang, Jun, Brian H. Toby, Peter L. Lee, Lynn Ribaud, Sytle M. Antao, Charles Kurtz, Mohan Ramanathan, Robert B. Von Dreele, and Mark A. Beno. 2008. "A Dedicated Powder Diffraction Beamline at the Advanced Photon Source: Commissioning and Early Operational Results." *Review of Scientific Instruments* 79 (8): 085105.

Wavefunction, Inc. 2020. *"Spartan '18" Version 1.4.5*. Wavefunction, Inc., Irvine, CA.

Wheatley, Austin M., and James A. Kaduk. 2019. "Crystal Structures of Ammonium Citrates." *Powder Diffraction* 34 (1): 35–43.